

To Find the Symmetry Plane in Any Dimension, Reflect, Register, and Compute a -1 Eigenvector

MARCELO CICONET, DAVID G. C. HILDEBRAND, AND HUNTER ELLIOTT

Image and Data Analysis Core
Harvard Medical School

May 5, 2022

Abstract

In this paper, we demonstrate that the problem of fitting a plane of reflection symmetry to data in any dimension can be reduced to the problem of registering two datasets, and that the exactness of the solution depends on the accuracy of the registration. The pipeline for symmetry plane detection consists of (1) reflecting the data with respect to an arbitrary plane, (2) registering the original and reflected datasets, and (3) finding the eigenvector of eigenvalue -1 of a matrix given by the reflection and registration mappings. Results are shown for 2D and 3D datasets. We discuss in detail a particular biological application in which we study the 3D symmetry of manual myelinated neuron reconstructions throughout the body of a larval zebrafish that were extracted from serial-section electron micrographs. The data consists of curves that are represented as sequences of points in 3D, and there are two goals: first, find the plane of mirror symmetry given that the neuron reconstructions are nearly symmetric; second, find pairings of symmetric curves.

I. PAPER OVERVIEW

- Section II: mathematical preliminaries and description of the method.
- Section III: quantitative experiments on 2D and 3D datasets.
- Section IV: description of a practical application for the field of neuroscience.
- Section V: literature review, and our method in perspective.
- Section VI: discussion of the method’s advantages, limitations, and possible future directions.

II. METHOD

Definition 1 (of Mirror Symmetry). *A set of points $P \subset \mathbb{R}^n$ is said to present mirror, reflection, or bilateral symmetry if there exists a hyper-plane $H \subset \mathbb{R}^n$ of dimension $n - 1$ such that the mirror reflection of P with respect to H produces a set of points Q such that $P = Q$.*

Definition 2 (of Mirror Reflection). *Let $H \subset \mathbb{R}^n$ be a $(n - 1)$ -dimensional hyper-plane, v a unit vector perpendicular to H , and p a fixed point in H , so that $H = \{q \in \mathbb{R}^n : \langle q - p, v \rangle = 0\}$. The mirror reflection of a set of points P with respect to H is the set $\{q - 2\langle q - p, v \rangle v : q \in P\}$.*

The mirror reflection with respect to a plane through the origin and with normal vector v is given by $x \mapsto S_v x$, where $S_v = I - 2vv^\top$, where I is the identity matrix. The reflection

with respect to a plane through an arbitrary point p and with normal vector v is given by:

$$x \mapsto S_{p,v}(x) = S_v x + 2dv,$$

where $d = \langle p, v \rangle$ is the “signed” distance between the plane and the origin. For simplicity of notation, we will henceforth replace $S_{p,v}(x)$ by $S_{p,v}x$.

The symmetry plane in \mathbb{R}^n can be computed in 3 steps, illustrated in Figure 1:

1. Reflect original data with respect to an arbitrary symmetry plane.
2. Register original and reflected sets.
3. Infer optimal symmetry plane from the parameters of the reflection and registration mappings.

The term “arbitrary” of step 1 only works in theory. In practice, it helps to start with a good guess for the actual symmetry plane, because the registration methods we used here are interactive optimization processes. Alternatively, we can try a number of different starts and pick the one for which the registration algorithm returns the most confident result. We use the former method for the application (Section IV), and the latter for the quantitative experiments (Section III).

There are two ways of performing step 3: one, by fitting a plane through the midpoints of pairs given by original and transformed data; two (the approach we adopt here), by solving an eigenvalue problem related to the global transformation

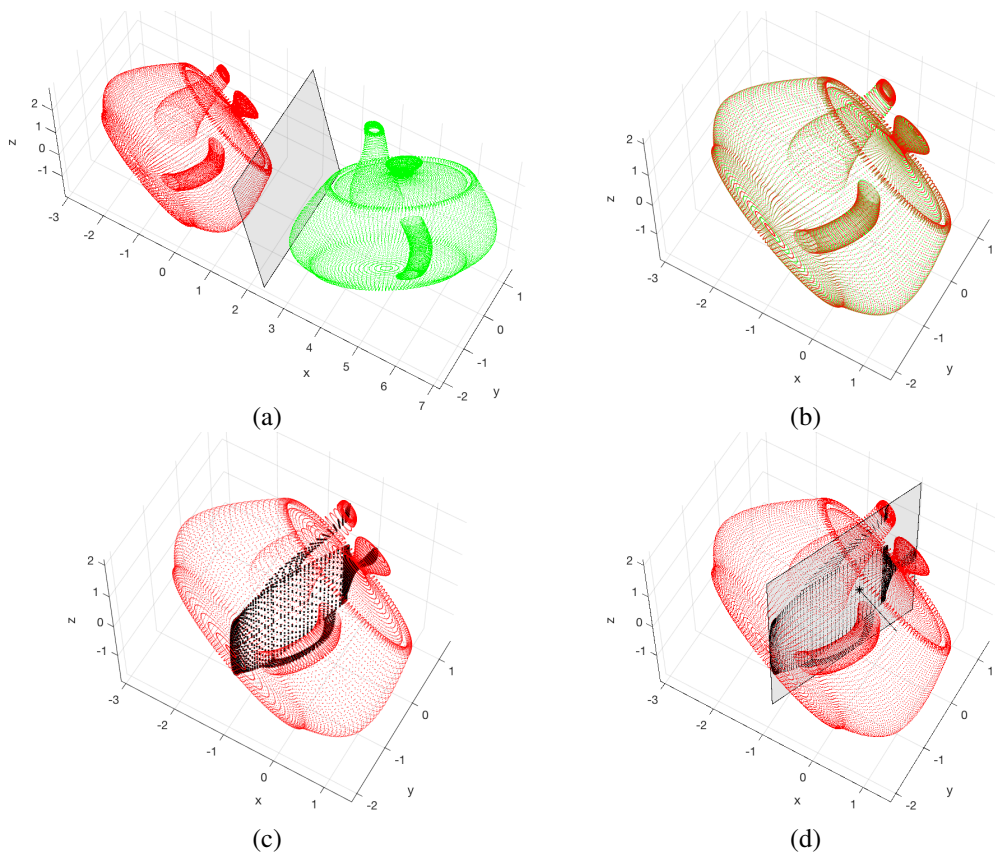


Figure 1: Symmetry plane detection in 3D. (a) The original data (in red) is reflected (reflection is shown in green) with respect to an initial plane – theoretically arbitrary, but in practice close to the estimated symmetry plane. (b) Registration between original and symmetric point clouds using the ICP algorithm. (c) Visualization of the midpoints (in black) between points in the original set and corresponding points on symmetric point cloud. (d) The symmetry plane can be computed either by fitting a plane to the midpoints in (c) or analytically as a solution to an eigenvalue problem on a function of the transformation matrices of the reflection and ICP registration mappings.

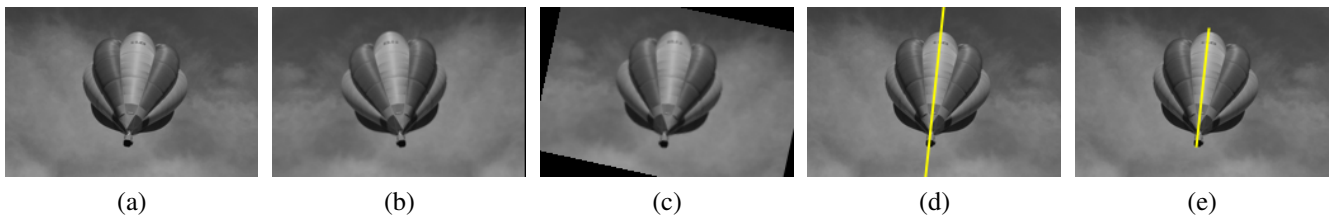


Figure 2: Symmetry line and segment detection in 2D. (a) Input image. (b) Reflection of the original image with respect to a vertical line through the center of the image. (c) Registration of (b) with respect to (a). (d) The symmetry line computed by the proposed algorithm is shown in yellow. (e) The symmetry segment is computed from (d) via a post-processing phase as described in [6].

(reflection and rigid transformation) that the original data went through.

We now introduce some mathematical facts that demonstrate why the pipeline works.

Let $P = \{p_1, \dots, p_N\}$ be a point cloud, and $Q = \{q_1, \dots, q_N\}$ the reflection of P given by $S_{p,v}$, that is, $q_i = S_{p,v}p_i \forall i$.

Proposition 1. *Let $m_i = \frac{1}{2}(p_i + q_i)$, so that $M = \{m_1, \dots, m_N\}$ is the set of midpoints between corresponding points in P and Q . Then the set M is contained in the plane with normal vector v passing through dv .*

Proof. For $x \in P$, the reflection by $S_{p,v}$ is $S_v x + 2dv$, and we have

$$\left\langle \frac{1}{2}(x + S_v x + 2dv) - dv, v \right\rangle = \quad (1)$$

$$\left\langle \frac{1}{2}x, v \right\rangle + \left\langle \frac{1}{2}S_v x, v \right\rangle + \langle dv, v \rangle - \langle dv, v \rangle. \quad (2)$$

But S_v is symmetric, so $\langle S_v x, v \rangle = \langle x, S_v v \rangle$. Further, $S_v v = -v$ because S_v is the reflection with respect to the plane through the origin with normal vector v , so $\langle x, S_v v \rangle = -\langle x, v \rangle$. Therefore (2) is equal to 0. \square

Let now R be the rigid transformation defined by $R(x) = R_0 x + t$, where R_0 is a rotation matrix and t a translation vector. If we reflect a point $x \in P$ by $S_{p,v}$ and then transform it through R , the result is $R_0(S_v x + 2dv) + t$.

Proposition 2. *Let $T = S_v R_0^\top$ and w equal the unit eigenvector of T corresponding to the eigenvalue -1 . That is, $Tw = -w$. (We will show in the next proposition that such w exists.) Let $r = \frac{1}{2}(R_0(2dv) + t)$, with d as previously defined. Then the midpoints $\frac{1}{2}(x + R_0(S_v x + 2dv) + t)$ lie in the plane with normal vector w passing through r .*

Proof.

$$\left\langle \frac{1}{2}(x + R_0(S_v x + 2dv) + t) - r, w \right\rangle = \quad (3)$$

$$\left\langle \frac{1}{2}(x + R_0(S_v x + 2dv) + t) - \frac{1}{2}(R_0(2dv) + t), w \right\rangle = \quad (4)$$

$$\frac{1}{2} \langle x + R_0(S_v x), w \rangle = \quad (5)$$

$$\frac{1}{2} (\langle x, w \rangle + \langle R_0 S_v x, w \rangle) = \quad (6)$$

$$\frac{1}{2} (\langle x, w \rangle + \langle x, S_v R_0^\top w \rangle) = \quad (7)$$

$$\frac{1}{2} (\langle x, w \rangle + \langle x, -w \rangle) = \quad (8)$$

$$0. \quad (9)$$

Proposition 3. *If S is a reflection and R is a rotation, then SR is a reflection. As a consequence, SR necessarily has -1 as an eigenvalue.*

Proof. Since S and R are orthogonal, so is SR . Further, since the determinant of the product equals the product of the determinants, the determinant of SR is -1 . Considering the reflection SR , let H be the reflection hyper-plane with normal vector v . In this case, $SRv = -v$, so v is the eigenvector of SR corresponding to the eigenvalue -1 . \square

Algorithm. Given the described method, the precise algorithm for finding the mirror symmetry plane for a set of points P is as follows:

1. Choose an initial reflection plane, given by a point p and a perpendicular vector v . For example, p can be the average (center of mass) of the points in P , and v the vector $(1, 0, \dots, 0)$.
2. Reflect all the points $x \in P$:

$$d = \langle p, v \rangle,$$

$$x \mapsto S_{p,v}x = S_v x + 2dv,$$

obtaining a new set of points Q .

3. Register Q to P through a rigid transformation, obtaining a rotation matrix R_0 and a translation vector t . (That is, the registration transformation is given by $x \mapsto R_0 x + t$.)
4. Compute the eigenvector \bar{v} of the matrix $S_v R_0^\top$ corresponding to the eigenvalue -1 . \bar{v} is the vector perpendicular to the symmetry plane.
5. Compute a point \bar{p} in the symmetry plane:

$$\bar{p} = \frac{1}{2}(R_0(2dv) + t).$$

A note on registration. All steps on the above pipeline are exact (when factoring out numerical errors), except for registration. If the data is not mirror symmetric, than the registration will not be precise. This approach shows that mirror symmetry can be reduced to a registration problem, with the robustness of the algorithm depending entirely on the robustness of the registration method.

III. QUANTITATIVE EXPERIMENTS

i. Metric

We tested the accuracy of our algorithm in 2D according to a previously introduced metric [14], which we now briefly

\square

describe. Let ϕ_G , c_G , and L_G be the angle, center point, and segment length, respectively, of the ground truth *segment* t_G . Let t_D be the segment proposed by the algorithm, with parameters ϕ_D , c_D , and L_D (analogous to ϕ_G , c_G , and L_G). Let $\Delta_{G,D}$ be the distance between the centers c_G and c_D . Segment t_D is considered to be a correct guess if

$$|\phi_G - \phi_D| < 10^\circ \text{ end } \Delta_{G,D} < \frac{1}{5} \min\{L_G, L_D\} .$$

Accuracy for *line* detection is measured in a similar fashion. Let now $\Delta_{G,D}^l$ be the distance between the *point* c_G (center of ground truth) and the *line* l_D . Line l_D is considered to correctly correspond to segment t_G if

$$|\phi_G - \phi_D| < 10^\circ \text{ end } \Delta_{G,D}^l < \frac{1}{5} L_G .$$

Notice that the distance between a line l_D and a segment t_G is never worse than the distance between a segment along a line, t_D , and the same segment t_G . This is because to estimate the distance between a line and a center, the center chosen along the line l_D is the closest one to the center c_G of the segment t_G .

In 3D, we evaluated accuracy by visual inspection of the projections of the data along three mutually perpendicular directions, one of which is perpendicular to the symmetry plane.

ii. Results

The state-of-the-art for single symmetry line/segment detection in 2D is a pairwise convolutional method [6], which we refer to here as CARS (Convolutional Approach to Reflection Symmetry). The authors of this method released the database used for tests, so we use the same dataset for testing our method (which we refer to as EIG, as in EIGenvalue, for lack of a better name¹).

Since our method outputs only lines, not segments, we post-process the symmetry line into segments using the same algorithm (even the same implementation) as CARS [6].

Accuracy and computation time comparisons are shown in Figure 5. We implemented two versions of the EIG algorithm based on two variants of registration methods: an intensity-based approach and a feature-based approach. These implementations relied on built-in MATLAB functions: *imregtform* for intensity-based, *pcregrigid* on binary edge maps of the images for feature-based. *pcregrigid* implements the Interactive Point Cloud (ICP) algorithm for point-cloud registration [5, 3]. To generate binary edge maps, we used the Ultrametric Contour Map [1] (see example in Figure 3).

¹“TFSPADRRRC-1E” is likely less memorable.

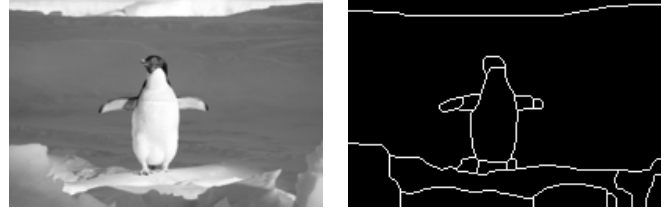


Figure 3: Binary edge maps produced by thresholding of the Ultrametric Contour Map [1] (right) for an example image (left).

Likely due to some clutter cleaning provided by the edge detection algorithm, performance for the feature-based registration approach performs better (68% for symmetry segment detection and 73% for symmetry line detection) than the intensity-based approach. In both cases, the EIG performance is worse than that reported for the CARS algorithm in its two variations, on the images and edge maps (Figure 5, top).

However, CARS is significantly more computationally expensive (Figure 5, bottom) due to its pairwise nature.

Furthermore, we did not experiment with all possible registration approaches. Beyond the two mentioned, we attempted to use SURF features in the feature-based approach, but results were not worth reporting. Since the accuracy of our method is directly related to the accuracy of the registration algorithm, a thorough study on registration approaches could be performed in case the chosen method is not accurate enough for a particular application. ICP worked nicely for our purposes (see Section IV).

We also used ICP as registration for a 3D symmetry plane detection experiment. To the best of our knowledge, there are no general-purpose symmetry detection databases for 3D bilateral symmetry detection tests. We hand-picked 203 symmetric 3D shapes from the McGill 3D Shape Benchmark [23]. Shapes include surface points of objects such as cups, airplanes, and insects.

By visual inspection, we verified that our method achieved 86% accuracy, i.e., correctly detected symmetry in 177 of 203 shapes. Some sample outputs are shown in Figure 4.

A note on initialization. Registration is typically an interactive optimization method, so it matters how close the chosen initial plane of symmetry is to the actual solution in step 1 of the algorithm. This can be done visually, when possible, as we did in our application (Section IV). For quantitative experiments, however, we applied the method on a few different guesses and used as the final solution the output whose registration algorithm confidence was higher. As initial guesses, we used hyper-planes centered at the origin with perpendicular

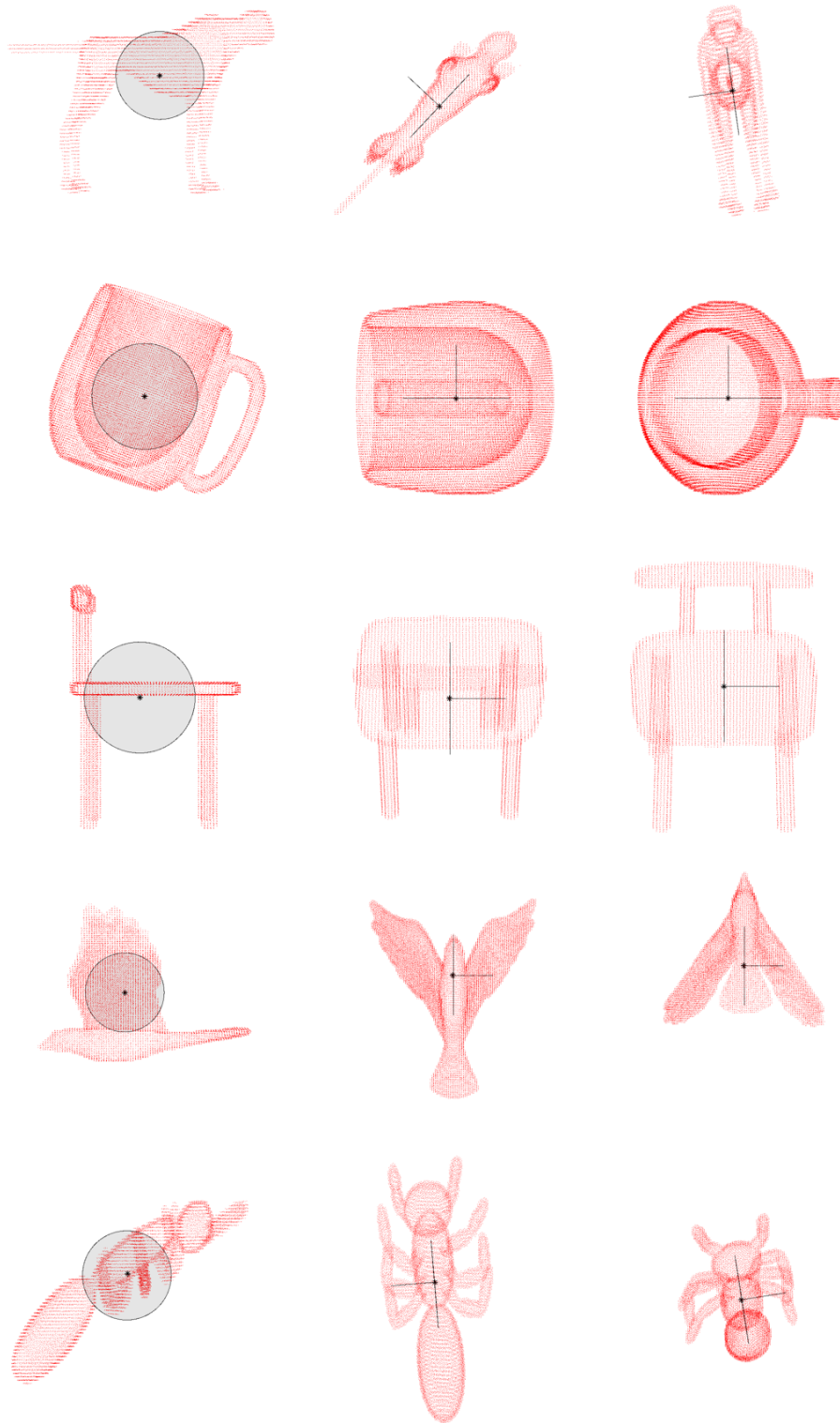


Figure 4: Sample 3D data from [23]. Each row contains different views of the same object. Views are projections of the data along three mutually perpendicular directions, one of which (left) is perpendicular to the symmetry plane.

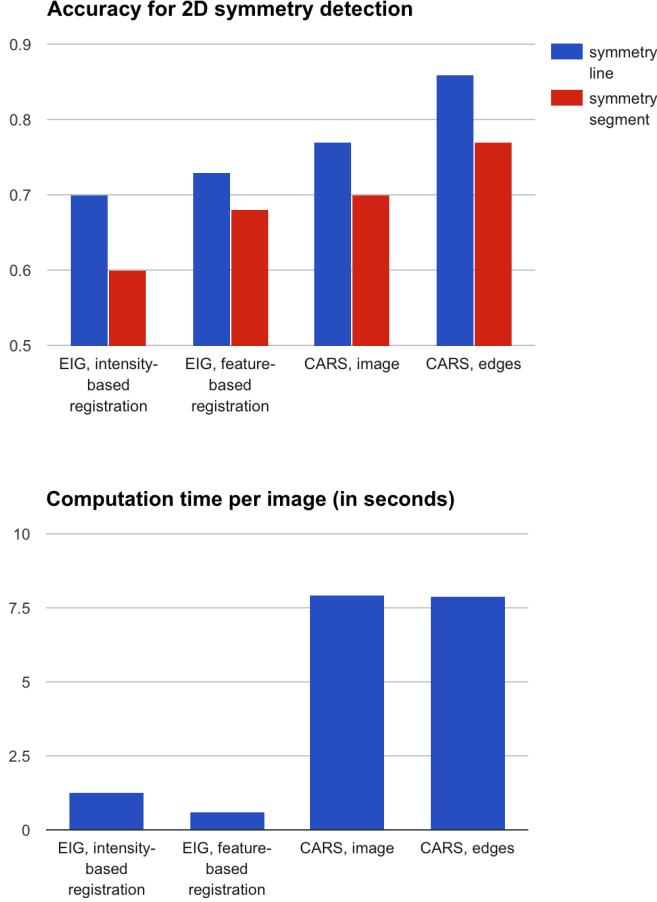


Figure 5: Top: Performance in 2D mirror symmetry detection of our EIG method versus the state-of-the-art CARS method. Bottom: Time comparison of computational cost of the evaluated methods as implemented in MATLAB.

vectors being those of the canonical basis of the respective space: $(1, 0)$ and $(0, 1)$ for \mathbb{R}^2 and $(1, 0, 0)$, $(0, 1, 0)$, $(0, 0, 1)$ for \mathbb{R}^3 .

IV. APPLICATION

This project was driven by a practical application in the field of neuroscience, in which we were interested in studying the 3D symmetry of manually reconstructed myelinated neuron projections throughout the body of a larval zebrafish that were extracted from serial-section electron micrographs. The data consists of curves represented as sequences of points in 3D, which are referred to as *skeletons*. There are two goals: first, find the plane of mirror symmetry given that the projections are nearly symmetric; and second, find pairings of symmetric

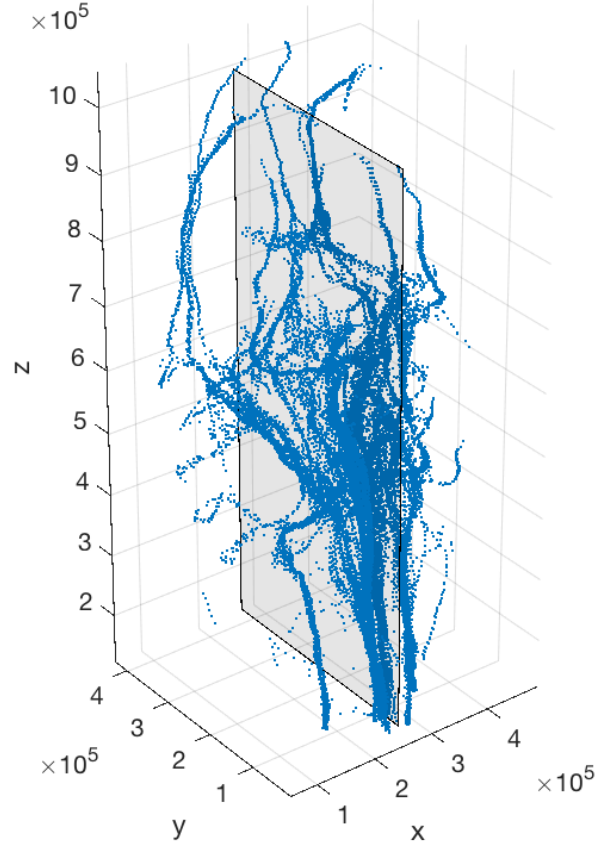


Figure 6: Myelinated neuron reconstructions (blue) from a larval zebrafish obtained through electron microscopy and the symmetry plane (transparent black) computed using the EIG approach.

skeletons.

Figure 6 shows the data, as well as the final symmetry plane computed with our method. Figure 7 shows the projection of the data along 3 mutually-perpendicular directions, one of which is perpendicular to the symmetry plane.

A skeleton s is a discrete curve in \mathbb{R}^n :

$$s = \{s_i : i = 1, \dots, n_s\}. \quad (10)$$

Given a reference symmetry plane H , a pairwise symmetry measure is computed by comparing one skeleton with the symmetric of the other with respect to H (Figure 8). Given two skeletons s and t , their similarity can be computed via Dynamic Time Warping (DTW), a variation of Dynamic Programming that is widely used for sequence matching [13].

Given a matrix of pairwise costs C , where $C(i, j) = C(j, i)$ is the symmetry measure between skeletons of indexes i and j , we apply the Munkres assignment algorithm (also known as the Hungarian method) [18] to compute the globally optimal

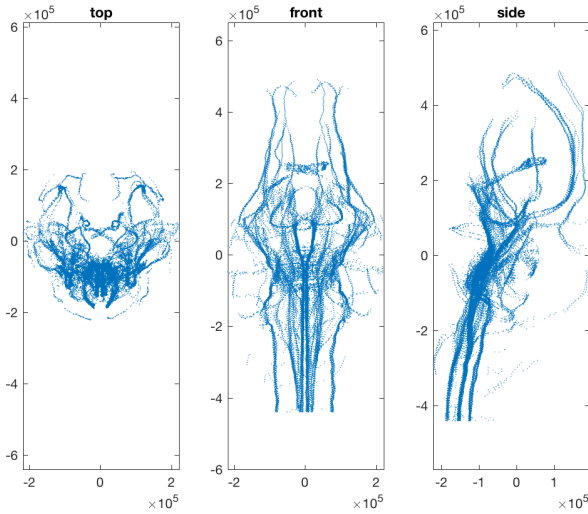


Figure 7: Projections of the data in Figure 6 along three mutually perpendicular directions, where the side projection is perpendicular to the symmetry plane.

pairwise assignment between skeletons.

This approach provides a new way to systematically compare and pair reconstructed neuronal projections in 3D. Assessing the degree to which every given projection pair is mirror symmetric makes it possible to identify new neuron types and neuronal pathways that exist bilaterally. This is important for finding specific anatomically defined neuron classes or brain regions that may share specific functional roles in sensation or behavior. Furthermore, analyzing the degree of symmetry in projections of previously identified neuron types will lend insights into the developmental processes that establish the projections and the system of which they are a part.

V. LITERATURE REVIEW

i. Mirror Symmetry Detection in 2D

2006. [15]: SIFT features were grouped into “symmetric constellations” by a voting scheme and the dominant symmetries presented in the image emerge as local maxima.

2012. [11]: Generalized reflection symmetry detection to a curved glide-reflection symmetry detection problem. Method estimates symmetry via a set of contiguous local straight reflection axes.

2013. [10]: 3-step algorithm; (1) correlation measures (using the SIFT descriptor) are computed along discrete directions; (2) symmetrical regions are identified by looking for matches in the directions characterized by maximum correlations; steps (1) and (2) are performed at different scales. [21]: 2-step algorithm; (1) candidates for mirror-symmetric patches are

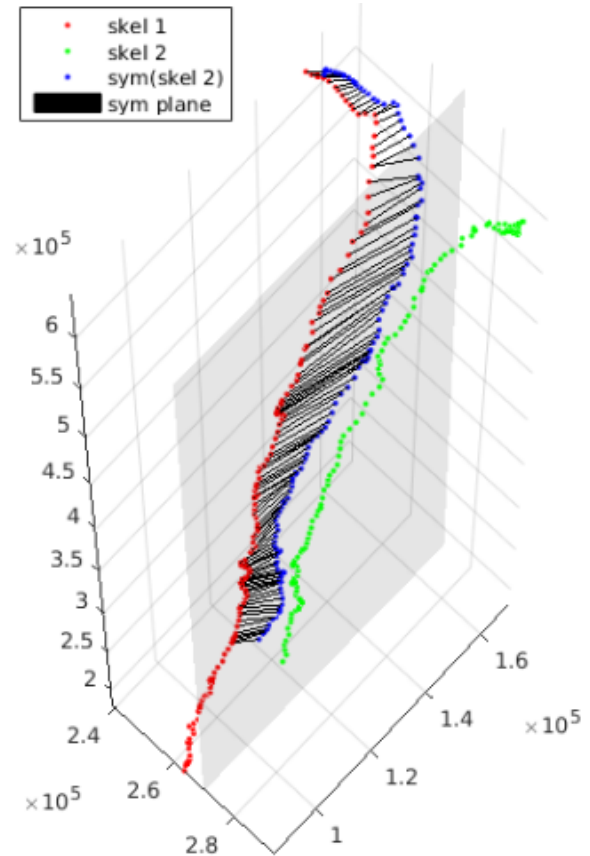


Figure 8: The symmetry matching cost for a skeleton pair is computed by measuring the DTW-distance between one skeleton and the symmetric (reflected) of the other with respect to the global symmetry plane.

identified using a Hough-like voting scheme; (2) candidates are validated using a principled statistical procedure inspired from a contrario theory. [16]: a combinatorial technique from Gestalt Algebra is used on top of SIFT descriptors. [14]: Evaluated different methods for symmetry detection in a common dataset, with [15] emerging as overall winner.

2014. [7]: Described a pairwise voting-scheme based on tangents computed via wavelet filtering. [4]: Presented an adaptive feature point detection algorithm to overcome clutter problems in feature-based methods for symmetry detection.

2015. [26]: Exhibited use of traditional edge detectors and a voting process, respectively, before and after a novel edge description and matching step based on locally affine invariant features.

2016. [6]: Described a pairwise convolutional approach to reflection symmetry, similar to [7]. The method outperformed [15] by a small margin. The authors released their own database, which we use here for testing. [8]: Exploited am-

ambiguities and challenges in symmetry detection to propose a ReCAPTCHA method based on symmetry.

ii. Mirror Symmetry Detection in 3D

1997. [25]: Converted symmetry detection problem to the correlation of the Gaussian image.

2002. [2]: Presented an approach similar to our method in its first 2 steps. However, the symmetry plane was fit on the set of midpoints, not obtained as the eigenvalue solution as presented here. Authors also did not include mathematical proofs for their results, and only conduct tests in 3D for symmetry in faces.

2006. [22]: Described a planar reflective symmetry transform that captures a continuous measure of the reflectional symmetry of a shape with respect to all possible planes. [20]: Presented a more robust version of a Gaussian image-based approach.

2011. [27]: Introduced a two step learning method with (1) landmark-related region detection; (2) symmetry plane computation in the learning stage that uses the landmarks and the standard symmetry planes identified by medical experts for training. [19]: Essentially mentioned [2] and reviewed ICP variations.

2013. [17]: Discussed applications in computer graphics and geometry that benefit from symmetry information for more effective processing. [9]: Described bilateral symmetry plane estimation for 3D shapes that is carried out in the spherical harmonic domain.

2014. [24]: Presented an algorithm that generates a set of candidate symmetries by matching local maxima of a surface function based on the heat diffusion in local domains, with a global optimum obtained by a voting scheme.

2015. [28]: Developed a skeleton-intrinsic shape symmetrization method accomplished by measuring intrinsic distances over a curve skeleton for symmetry analysis, symmetrizing the skeleton, and then propagating the symmetrization from skeleton to shape.

2016. [12]: Achieved symmetry plane detection by first generating a candidate symmetry plane based on a matching pair of sample views and then verifying whether the number of remaining matching pairs is within a minimum number.

iii. Mirror Symmetry Detection in \mathbb{R}^n

We are unaware of a previous work claiming to devise a mirror symmetry detection method that is invariant to the dimension of the space.

VI. CONCLUSION

We introduce a mirror symmetry detection method with the following qualities:

- Invariance to dimension. Experiments were shown for 2D and 3D datasets.
- Mathematically exactness (except for a data registration phase). We prove that mirror symmetry detection in \mathbb{R}^n can be as good as the best available registration method.
- Computationally fast.

Our method presents the following limitations:

- Restricted to single-plane symmetry applications (i.e., only finds one symmetry plane).
- Lacks output for the intersection of the symmetry hyperplane with the symmetric object. In 2D, for example, it only outputs the symmetry line, not the symmetry segment – a segment output would be more useful as an aid to object detection, for instance.

To highlight the importance of mirror symmetry detection, we discussed a study of 3D symmetry in myelinated neuronal projections of a larval zebrafish. Measuring mirror symmetry between skeleton pairs made it possible to identify neuron types and revealed neuronal projections that are arranged bilaterally. This is important for finding specific anatomically defined neuron classes or brain regions that may share specific functional roles in sensation or behavior.

An immediate direction for future work is an extension that allows detection of multiple symmetry planes. On the theoretical side, a better metric on the space of planes in \mathbb{R}^n should be developed to more adequately measure accuracy.

REFERENCES

- [1] P. Arbelaez, M. Maire, C. Fowlkes, and J. Malik. Contour detection and hierarchical image segmentation. *IEEE Trans. Pattern Anal. Mach. Intell.*, 33(5):898–916, May 2011.
- [2] M. Benz, X. Laboureaux, T. Maier, E. Nkenke, S. Seeger, F. W. Neukam, and G. Häusler. The symmetry of faces. In *Proceedings of the Vision, Modeling, and Visualization Conference 2002 (VMV 2002), Erlangen, Germany, November 20-22, 2002*, pages 43–50, 2002.
- [3] P. J. Besl and N. D. McKay. A method for registration of 3-d shapes. *IEEE Trans. Pattern Anal. Mach. Intell.*, 14(2):239–256, 1992.
- [4] D. Cai, P. Li, F. Su, and Z. Zhao. An adaptive symmetry detection algorithm based on local features. In *Visual Communications and Image Processing Conference, 2014 IEEE*, pages 478–481, Dec 2014.

- [5] Y. Chen and G. G. Medioni. Object modelling by registration of multiple range images. *Image Vision Comput.*, 10(3):145–155, 1992.
- [6] M. Cicconet, V. Birodkar, M. Lund, M. Werman, and D. Geiger. A convolutional approach to reflection symmetry. <http://arxiv.org/abs/1609.05257>, 2016. New York.
- [7] M. Cicconet, K. Gunsalus, D. Geiger, and M. Werman. Mirror symmetry histograms for capturing geometric properties in images. *CVPR*, 2014. Columbus, Ohio.
- [8] C. Funk and Y. Liu. Symmetry recaptcha. In *The IEEE Conference on Computer Vision and Pattern Recognition (CVPR)*, June 2016.
- [9] R. Kakarala, P. Kaliamoorthi, and V. Premachandran. Three-dimensional bilateral symmetry plane estimation in the phase domain. In *2013 IEEE Conference on Computer Vision and Pattern Recognition, Portland, OR, USA, June 23-28, 2013*, pages 249–256, 2013.
- [10] S. Kondra, A. Petrosino, and S. Iodice. Multi-scale kernel operators for reflection and rotation symmetry: Further achievements. In *Computer Vision and Pattern Recognition Workshops (CVPRW), 2013 IEEE Conference on*, pages 217–222, June 2013.
- [11] S. Lee and Y. Liu. Curved glide-reflection symmetry detection. *Pattern Analysis and Machine Intelligence, IEEE Transactions on*, 34(2):266–278, Feb 2012.
- [12] B. Li, H. Johan, Y. Ye, and Y. Lu. Efficient 3d reflection symmetry detection: A view-based approach. *Graphical Models*, 83:2–14, 2016.
- [13] S. Z. Li and A. Jain, editors. *Dynamic Time Warping (DTW)*, pages 231–231. Springer US, Boston, MA, 2009.
- [14] J. Liu, G. Slota, G. Zheng, Z. Wu, M. Park, S. Lee, I. Rauschert, and Y. Liu. Symmetry detection from real world images competition 2013: Summary and results. *CVPR Workshop*, 2013. Portland, Oregon.
- [15] G. Loy and J.-O. Eklundh. Detecting symmetry and symmetric constellations of features. In *Proceedings of the 9th European Conference on Computer Vision - Volume Part II, ECCV'06*, pages 508–521, Berlin, Heidelberg, 2006. Springer-Verlag.
- [16] E. Michaelsen, D. Muench, and M. Arens. Recognition of symmetry structure by use of gestalt algebra. In *Computer Vision and Pattern Recognition Workshops (CVPRW), 2013 IEEE Conference on*, pages 206–210, June 2013.
- [17] N. J. Mitra, M. Pauly, M. Wand, and D. Ceylan. Symmetry in 3d geometry: Extraction and applications. *Comput. Graph. Forum*, 32(6):1–23, 2013.
- [18] J. Munkres. Algorithms for the assignment and transportation problems. *Journal of the Society for Industrial and Applied Mathematics*, 5(1):32–38, 1957.
- [19] C. Padia and N. Pears. A review and characterization of icp-based symmetry plane localisation in 3d face data. Technical report, Department of Computer Science, University of York, UK, 2011.
- [20] G. Pan, Y. Wang, Y. Qi, and Z. Wu. Finding symmetry plane of 3d face shape. In *18th International Conference on Pattern Recognition (ICPR 2006), 20-24 August 2006, Hong Kong, China*, pages 1143–1146, 2006.
- [21] V. Patraucean, R. von Gioi, and M. Ovsjanikov. Detection of mirror-symmetric image patches. In *Computer Vision and Pattern Recognition Workshops (CVPRW), 2013 IEEE Conference on*, pages 211–216, June 2013.
- [22] J. Podolak, P. Shilane, A. Golovinskiy, S. Rusinkiewicz, and T. A. Funkhouser. A planar-reflective symmetry transform for 3d shapes. *ACM Trans. Graph.*, 25(3):549–559, 2006.
- [23] K. Siddiqi, J. Zhang, D. Macrini, A. Shokoufandeh, S. Bouix, and S. Dickinson. Retrieving articulated 3-d models using medial surfaces. *Mach. Vision Appl.*, 19(4):261–275, May 2008.
- [24] I. Sipiran, R. Gregor, and T. Schreck. Approximate symmetry detection in partial 3d meshes. *Comput. Graph. Forum*, 33(7):131–140, 2014.
- [25] C. Sun and J. Sherrah. 3d symmetry detection using the extended gaussian image. *IEEE Trans. Pattern Anal. Mach. Intell.*, 19(2):164–168, 1997.
- [26] Z. Wang, Z. Tang, and X. Zhang. Reflection symmetry detection using locally affine invariant edge correspondence. *Image Processing, IEEE Transactions on*, 24(4):1297–1301, April 2015.
- [27] J. Wu, R. Tse, C. L. Heike, and L. G. Shapiro. Learning to compute the plane of symmetry for human faces. In *Proceedings of the 2Nd ACM Conference on Bioinformatics, Computational Biology and Biomedicine, BCB '11*, pages 471–474, New York, NY, USA, 2011. ACM.
- [28] Q. Zheng, Z. Hao, H. Huang, K. Xu, H. Zhang, D. Cohen-Or, and B. Chen. Skeleton-intrinsic symmetrization of shapes. *Comput. Graph. Forum*, 34(2):275–286, 2015.